Enhancement of solidification of PCM around finned tubes: modeling and validation

Kamal A. R. Ismail[1], Priscilla D. da Silva[2], Fatima A. M. Lino[3]

[1,2,3] State University of Campinas, Faculty of Mechanical Engineering, Department of Energy, Mendeleiev street, 200, Postal Code 13083-860, Cidade Universitária "Zeferino Vaz", Barão Geraldo, Campinas, SP, Brazil

Abstract: - Phase change materials (PCMs) are the most attractive thermal energy storage media due to their reduced storage volume and isothermal behavior during charging and discharging processes. Their main drawback is the slow thermal response due to the low thermal conductivity. Various methods for PCM thermal conductivity enhancement have been investigated by many researchers. The present study has the objective of investigating fins for enhancing thermal conductivity of PCM and meliorates their thermal performance. The formulated model for the horizontal radial finned tube is based on pure conduction in the PCM and numerically treated by finite difference and Alternating Direction Implicit (ADI) formulation. The numerical code is optimized and the numerical predictions were validated against experimental results. Additional numerical and experimental measurements were realized to investigate the effects of the cooling fluid temperature, its mass flow rate, diameter, thickness and material of the fin on the interface velocity, solidified mass and the time for complete solidification.

Keywords: - *Finned tube, latent heat storage system, PCM, phase change, solidification, thermal conductivity enhancement*

I. INTRODUCTION

Phase change materials (PCMs) are attractive as thermal energy storage media due to their high thermal capacity and their isothermal behavior during the phase change processes compared with sensible heat storage systems. However, latent heat storage technology is still not widely implemented in practical applications because of the difficulty to find PCM that possesses high thermal conductivity, large latent heat, low super cooling and good stability among other characteristics. Organic PCMs are good candidates but have slow thermal response due to their low thermal conductivity. Therefore, effective enhancement methods for the liquid–solid phase change are the key issue that limits their practical application in latent heat energy storage technology. Some works are worth mentioning because they treated certain aspects of the phase change process in the early developments stages as [1, 2, 3]. Henze and Humphrey [1] presented a simplified numerical model based on a quasi-linear transient equation, which predicts the fraction of melted PCM, and the shape of the liquid-solid interface as a function of time with sufficient accuracy for engineering purposes. Experimental results were compared with model predictions, and fairly good agreement was found. On the other hand, Padmanabhan and Murthy [2] presented a numerical study for the phase change process occurring in a cylindrical annulus in which rectangular, uniformly spaced axial fins, spanning the annulus are attached to the inner isothermal tube. The time-wise evolution of the interface profile, phase-change fraction and energy stored/discharged were presented. Later, Ismail et al. [3] presented the results of a numerical and experimental investigation on finned tubes. The model was based upon the pure conduction, the enthalpy formulation approach and the control volume method. Their results were validated against available results and their own experimental measurements. The number of fins, fin length, fin thickness, the degree of super heat and the aspect ratio of the annular spacing were found to influence the time for complete solidification, solidified mass fraction and the total stored energy.

Ismail and Silva [4] presented the results of a numerical study on melting of PCM around a horizontal circular cylinder in the presence of the natural convection in the melt phase. A two dimensional unsteady model was formulated in terms of primitive variables and a coordinate transformation technique has been used to fix the moving front. The finite volume approach was used to discretize the system of governing equations, boundary and initial conditions. The numerical predictions were compared with available results to establish the validity of the model and the numerical approach.

Liu et al. [5] studied experimentally the performance of a thermal storage unit using stearic acid as the heat storage medium. The thermal performance of the unit was measured, and the heat transfer characteristics of the melting process were studied under different heat flux conditions to determine the influence of heat flux on the melting processes. It was shown that the fin effectively improved both heat conduction and natural convection.

A numerical and experimental investigation was realized by Kayansayan and Acar [6] on a cold thermal energy storage system involving phase-change process dominated by heat conduction. The problem involved a fluid flowing inside a horizontal finned tube surrounded by PCM. Comparison between the numerical predictions and the experimental data showed good agreement.

Yuksel et al. [7] proposed a theoretical approach for the prediction of time and temperature during phase change in the latent heat storage. By the use of the average values of the mean specific heat capacities for the phase-changed materials, analytical solutions are obtained and compared with the available experimental data in the literature. The agreement between the theoretical model results and the experimental data was good.
A different approach to enhance thermal conductivity of the PCM was investigated by Jegadheeswaran and Pohekar [8]. They presented the results of a numerical study to investigate the performance enhancement of a latent heat storage unit of shell and tube configuration due to the dispersion of high conductivity particles in the PCM during charging process. Temperature based governing equations have been formulated and solved numerically following an alternate iteration between the temperature and thermal resistance. The results indicate a significant improvement in the performance of the latent heat storage unit when high conductivity particles are dispersed. Later, Chintakrinda et al. [9] analyzed the thermal performance and energy storage capabilities of a 54 ^{o}C organic paraffin wax and directly compared using three common different thermal conductivity enhancement methods including the use of graphite foam with infiltrated PCM, aluminum foam with infiltrated PCM, and PCM with 10 wt% graphite nano-fibers. It was found that the selection of enhancement method has a significant effect on the thermal response of the system.

The concept of storage of any type of energy can have a positive impact on greenhouse gas (GHG) emissions. The urgent need to control GHG emissions and better use of energy and other resources can boost up and extends the applicability of PCM to other areas. Anisur et al. [10] emphasized the opportunities for energy savings and GHG emissions reduction with the implementation of PCM in TES systems. About 3.43% of CO_2 emission by 2020 could be reduced through the application of PCM in building and solar thermal power systems. Similarly, energy conservation and GHGs emission reduction by other PCM applications for thermal comfort of vehicles, transport refrigeration, greenhouse and waste heat management are also presented.

Rahimi et al. [11] conducted an experimental study to investigate melting and solidification processes of paraffin RT35 as phase change materials in a finned-tube. It was shown that, using fins in phase change process enhances melting and solidification processes.

Ismail et al. [12] presented the results of a numerical study on internally and externally finned annulus in which the internal tube has external fins while the external tube has internal fins. This arrangement was investigated with the objective of increasing the heat transfer rate, reducing the time for complete phase change and allowing for simultaneous charging and discharging processes. The proposed model was based upon pure conduction and its validity was established by comparison with available data. In another work Ismail et al. [13] presented the results of an investigation on axially finned tubes to enhance the processes of charging and discharging thermal storage units. The proposed model was based upon pure conduction in the solid and liquid phases. The enthalpy approach and the finite volume method were used in the numerical treatment. The numerical predictions were compared with experimental results and relatively good agreement was observed.

The main objective of the present paper is to investigate the effect of radially finned tube on the enhancement of solidification and reduction of time for complete solidification during the phase change process. A pure conduction model was formulated and solved by finite difference. The numerical predictions and method of solution were validated against experimental results showing reasonably good agreement.

II.   FORMULATION OF THE MODEL

The present problem treats the solidification of PCM inside a storage tank of the latent heat type composed of a bundle of horizontal tubes fitted with radial fins and extending along the length of the storage tank. Since the objective of the investigation is to study the process of phase change around tubes with radial fins, a representative section of this configuration which is composed of the finned tube surrounded by a symmetry circle and extending from entry to exit along the storage tank is shown in Fig. 1. The symmetry circle is defined as the limiting boundary beyond which there is no heat transfer or phase change. The PCM is placed in the space between the finned tube and the boundary of the symmetry circle while the cold cooling fluid flows inside the finned tubes solidifying the PCM externally around them. Fig. 1 shows a general layout of the problem and the instantaneous interface between the solidified and the liquid PCM.
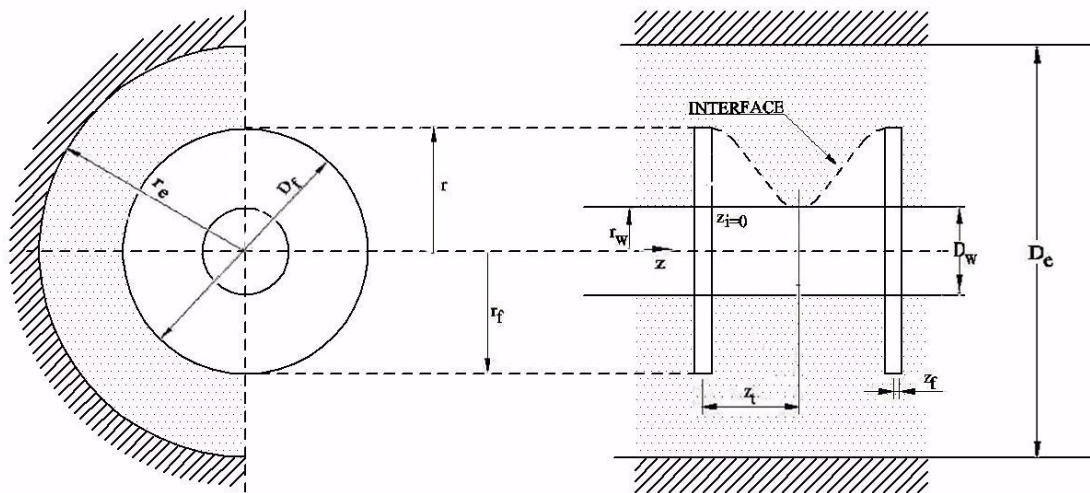
Fig. 1 Sketch of the problem of phase change around a finned tube.

In order to formulate the model a two dimensional coordinate system is used, where the z direction is along the finned tube axis and the radial coordinate is along the radial direction. Some assumptions are admitted to be able to formulate the model. For example, the PCM is considered as a pure substance, incompressible, has constant phase change temperature, and initially in the liquid fase. The physical properties such as density, specific heat and thermal conductivity of the solid and liquid phases are known. The mechanism of heat exchange during the phase change process is controlled by pure conduction and convection in the PCM liquid phase is neglected.

At any instant, one can write the governing equations and the associated boundary conditions in cylindrical coordinates as the energy equation of the solid PCM is

$$\rho_s c_s \frac{\partial T_s}{\partial t} = \frac{1}{r}\frac{\partial}{\partial r}\left(rk_s \frac{\partial T_s}{\partial r}\right) + \frac{\partial}{\partial z}\left(k_s \frac{\partial T_s}{\partial r}\right) \tag{1}$$

the energy equation of the liquid PCM

$$\rho_l c_l \frac{\partial T_l}{\partial t} = \frac{1}{r}\frac{\partial}{\partial r}\left(rk_l \frac{\partial T_l}{\partial r}\right) + \frac{\partial}{\partial z}\left(k_l \frac{\partial T_l}{\partial r}\right) \tag{2}$$

the boundary conditions at the solid / liquid interface

$$\left(k_s \frac{\partial T_s}{\partial r} - k_l \frac{\partial T_l}{\partial r}\right)\left(1 + \left(\frac{\partial s}{\partial z}\right)^2 \right) = \rho_s L \frac{\partial s}{\partial t} \tag{9}$$

$$T_s = T_l = T_m \qquad r = s(t) \tag{10}$$

boundary condition at the wall of the tube

$$r = r_w \qquad\qquad T = T_w \tag{11}$$

boundary condition at the symmetry circle

$$r = r_e \qquad\qquad \frac{\partial T}{\partial r} = 0 \tag{12}$$

boundary condition at the tube entrance section

$$z = z_i \qquad\qquad \frac{\partial T}{\partial z} = 0 \tag{13}$$

boundary condition at the tube exit section

$$z = z_t \qquad\qquad \frac{\partial T}{\partial z} = 0$$

the initial and final conditions can be written as

$$T(r, z, t_{=0}) = T_m + \Delta T$$

$$T(r, z, t_f) = T_m - \Delta T \tag{14}$$

where ΔT is half of the phase change temperature range.

The enthalpy of the PCM per unit volume, Bonacina et al. [14], can be written as:

$$H(T) = \int_T C(T)\,dT + \lambda\,\eta\,(T - T_m) \tag{15}$$

where

$C(T)$: Specific heat per unit volume;

λ: Latent heat of solidification;

η: Unit step function.

the thermal capacity per unit volume can be defined as:

$$\overline{C}(T) = \frac{dH(T)}{dT} = C(T) + \lambda\,\delta(T - T_m) \tag{16}$$

Where $\delta(T - T_m)$ is the Dirac delta fuction and

$$C(T) = \begin{cases} C_s(T) & T < T_m - \Delta T \\ C_l(T) & T > T_m + \Delta T \end{cases} \tag{17}$$

Where C_s and C_l are the thermal capacities in the solid and liquid phases, respectively.

Substituting eq. 16 into eq. 15 one can obtain the equivalent thermal capacity per unit volume integrated over the phase change range as

$$H(T) = \int_{T_m - \Delta T}^{T_m + \Delta T} C(T)\,dT = \lambda + \int_{T_m - \Delta T}^{T_m} C_s(T)\,dT + \int_{T_m}^{T_m + \Delta T} C_l(T)\,dT \tag{18}$$

the thermal conductivity can be written in a similar manner as

$$\overline{k}(T) = \begin{cases} k_s(T) & T \leq T_m - \Delta T \\ k_l(T) & T \geq T_m - \Delta T \end{cases} \tag{19}$$

Considering that C_s and C_l do not depend on the phase change temperature range and that k_s and k_l change linearly in the phase change temperature range one can write:

$$\overline{C}(T) = \begin{cases} C_s(T); & T \leq T_m - \Delta T \\ C_l(T); & T \geq T_m + \Delta T \\ \dfrac{\lambda}{2\Delta T} + \dfrac{C_s(T) + C_l(T)}{2}; & T_m - \Delta T < T < T_m + \Delta T \end{cases} \tag{20}$$

$$\overline{k}(T) = \begin{cases} k_s(T); & T \leq T_m - \Delta T \\ k_l(T); & T \geq T_m + \Delta T \\ k_l(T) + \dfrac{k_l(T) - k_s(T)}{2\Delta T}\left(T - (T_m - \Delta T)\right); & T_m - \Delta T < T < T_m + \Delta T \end{cases} \tag{21}$$

where

$$C_s = \rho_s c_s$$
$$C_l = \rho_l c_l \tag{22}$$
$$\lambda = \rho_s L$$

Using eqs. 20-22 with eqs.1 and 2 the energy equations of the solid and liquid phases as well as the phase interface equation can be expressed in a single form as in eq. 23.

$$\overline{C}(T)\frac{\partial T}{\partial t} = \frac{1}{r}\frac{\partial}{\partial r}\left(r\overline{k}(T)\frac{\partial T}{\partial r}\right) + \frac{\partial}{\partial z}\left(\overline{k}(T)\frac{\partial T}{\partial z}\right) \tag{23}$$

When using eq. 24 for the fin the fin thermal properties must be used, that is

$$\overline{C}(T) = \rho_f c_f = C_f$$
$$\overline{k}(T) = k_f$$

(24)

To facilitate the numerical calculations eq. 23 and the associated boundary, initial and final conditions are expressed in dimensionless form by using the following dimensionless parameters and variables

$$\varphi = \frac{T - T_r}{(T_m + \Delta T) - T_r}; \quad R = \frac{r}{r_w};$$

$$\overline{k} = \frac{k}{k_s}; \qquad\qquad \overline{C} = \frac{C}{C_s};$$

$$\tau = \frac{k_s t}{C_s r_w^2}; \qquad\qquad C_{ls} = \frac{C_l}{C_s};$$

$$k_{ls} = \frac{k_l}{k_s}; \qquad\qquad Ste_{\Delta T} = \frac{C_s \Delta T}{\rho_s L} = \frac{C_s \Delta T}{\lambda};$$

$$C_{fs} = \frac{C_f}{C_s}; \qquad\qquad \xi = \frac{\Delta T}{T_m - T_w};$$

$$k_{fs} = \frac{k_f}{k_s}; \qquad\qquad Z = \frac{z}{r_w}$$

(25)

eq. 23 in terms of the new variables is

$$\overline{C}(\phi)\frac{\partial \phi}{\partial \tau} = \frac{1}{R}\frac{\partial}{\partial R}\left(R\,\overline{k}(\phi)\frac{\partial \phi}{\partial R}\right) + \frac{\partial}{\partial Z}\left(\overline{k}(\phi)\frac{\partial \phi}{\partial Z}\right)$$

(26)

while the boundary conditions become
tube wall:

$$\phi_w = 0 \qquad R = 1$$

symmetry circle:

$$\frac{\partial \phi}{\partial R} = 0 \qquad R = R_e$$

(27)

initial interface position:

$$\frac{\partial \phi}{\partial Z} = 0 \qquad Z = Z_i = 0$$

final interface position:

$$\frac{\partial \phi}{\partial Z} = 0 \qquad Z = Z_t$$

Initial and final conditions are respectively:

$$\phi = 1$$
$$\phi = 1 - 2\xi$$

(28)

The set of equations of the model and the boundary and initial conditions were implemented in a computational code. Experimental tests were realized to ensure that the results are independent of the choice of the number of grid points. The grid points which make the results independent according to the numerical tests is found to be 45 along the tube while the number of grid points along the radial fin is taken as 33 points. The time step is taken as 10^{-3} s. These values are used in all the numerical simulations.

III. EXPERIMENTAL ANALYSIS

In order to validate the model and the numerical predictions an experimental set up is constructed and instrumented as shown in Fig. 2. The test set up is composed of a compression refrigerant circuit, secondary fluid circuit, coiled tube heat exchanger submersed in the secondary fluid tank, the test section of the finned tube which is connected to the secondary fluid circuit. The secondary fluid is Ethanol cooled by the refrigerant flowing through the coiled tube heat exchanger and its temperature and mass flow rate are controlled as required.

The test section is of rectangular shape built from 15 mm thick acrylic sheet with the test tube extended across the test section filled with PCM (water) whose initial temperature can be varied as desired. High resolution digital camera is used to photograph the finned tube and the reference scale to be used to convert the image dimensions to real values as will be explained later. Calibrated thermocouples type K, are fixed at entry and exit of the finned tube, in the PCM test tank, along the finned tube and in the secondary fluid tank. The thermocouples were calibrated to within ± 0.5 °C, image conversion precision to within ± 0.1mm while the mass flow rate (measured by a calibrated orifice plate) to within $\pm 10^{-4}$ kg/s.

Measurements were usually taken when the desired testing conditions were achieved, that is the temperature of the working fluid in the finned tube, temperature of the Ethanol tank, temperature of the PCM, and the mass flow rate of the secondary fluid. Under these initial conditions the chronometer is started after all initial conditions are registered. During the first two hours each 5 minutes period all measurement points are registered and a photograph of the finned tube is taken. During the third hour measurements are registered each 15 minutes interval. After that the time interval is increased to 30 minutes until the end of the test. The test is considered terminated when no change in temperature or interface position is registered during three successive time intervals.

A typical photograph of the finned tube is shown in Fig. 3 where the interface position is tracked and converted to real dimension by using the program Tracker as shown in Fig. 4.
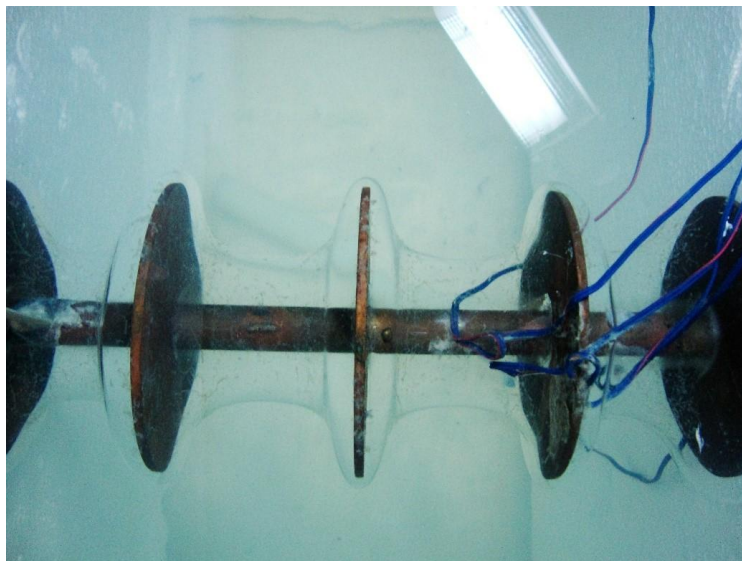

Fig. 2 The experimental installation.

Fig. 3 The finned tube, the solidified PCM and the thermocouples for temperature measurements.
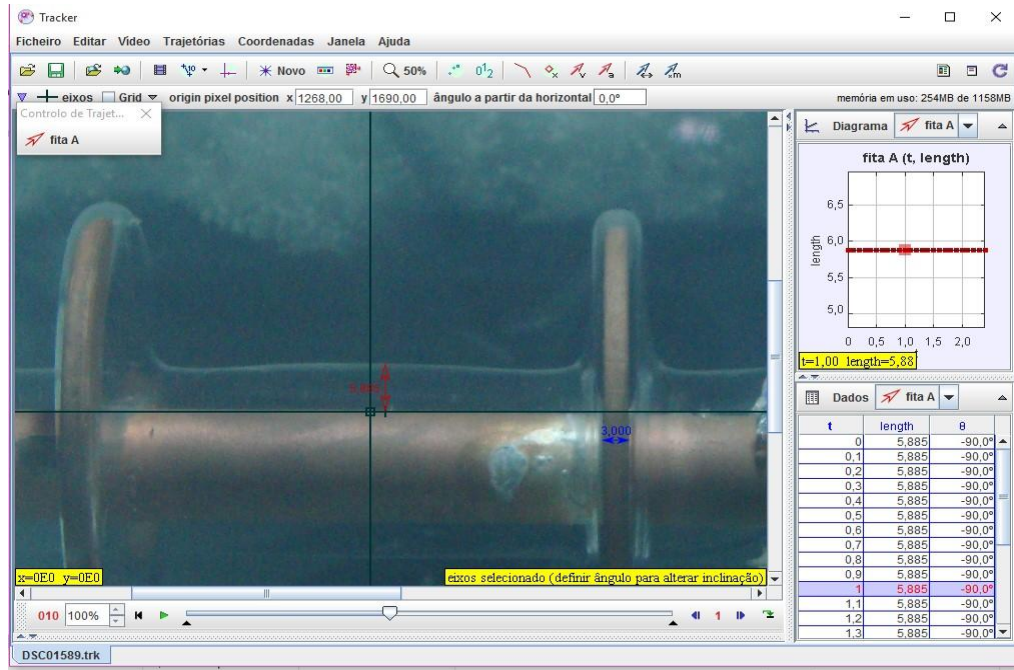
Fig. 4 Tracker software with the finned tube positioned for digitalization of the interface position.

IV.   RESULTS AND DISCUSSION
4.1 VALIDATION OF THE RESULTS

The model and the numerical predictions were validated against experiments conducted by the authors. Fig. 5 shows a comparison between the numerical predictions of the interface velocity and the experimental measurements for the case of tube with 95 mm fin diameter. As can be seen the agreement is good. Fig. 6 shows a similar comparison for the case of fin with 75 mm diameter indicating a relatively good agreement.

Comparative results for the solidified mass fraction are shown in Figs. 7-8. Fig. 7 shows a comparison of the predicted solidified mass fraction and the experimentally determined mass fraction. As can be seen the agreement is very good and hence confirming the suitability of the model and the method of solution to handle the problem of solidification around finned tubes.
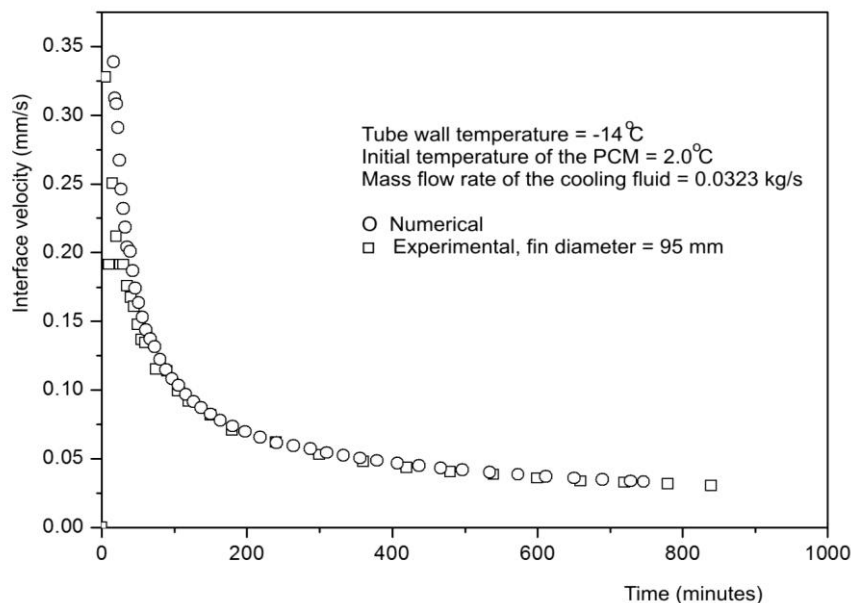
Fig. 5 Numerical and experimental comparison of the instantaneous interface velocity for a finned tube of 95 mm diameter.
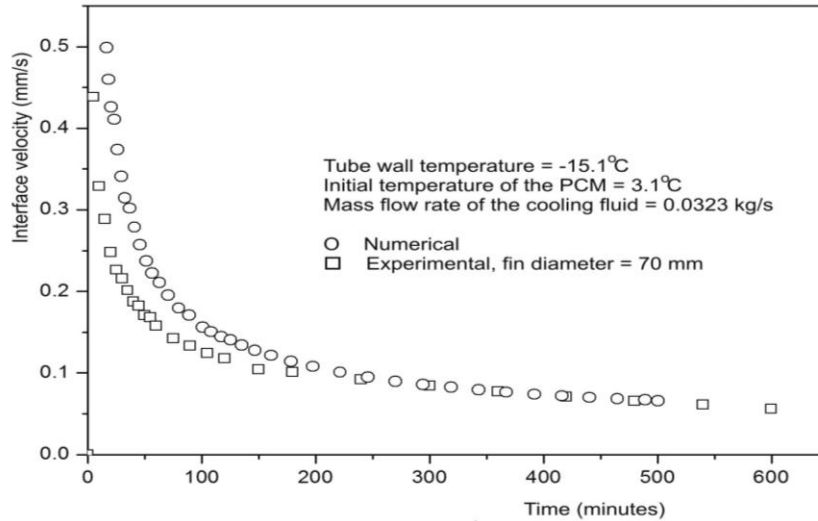
Fig. 6 Numerical and experimental comparison of the instantaneous interface velocity for a finned tube of 70 mm diameter.
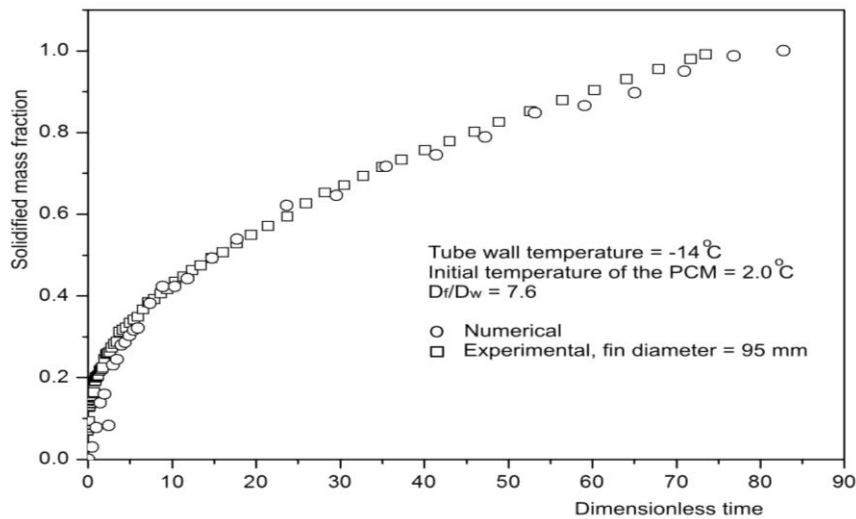

Fig. 7 Numerical and experimental comparison of the solidified mass fraction against dimensionless time for a finned tube of 95 mm diameter.
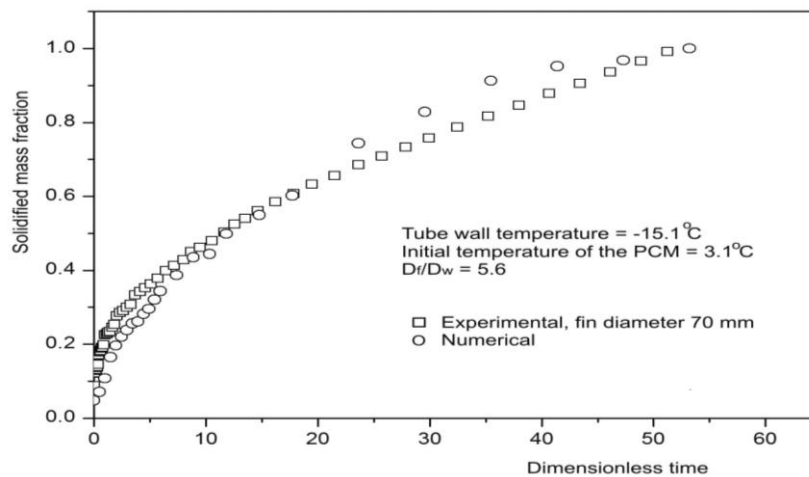

Fig. 8 Numerical and experimental comparison of the solidified mass fraction against dimensionless time for a finned tube of 70 mm diameter.

Fig. 8 shows a similar comparative result for the case of tube with 70 mm fin diameter. As can be seen the agreement is relatively good except in the final part of the process where the experimental results are lower values due to possible losses from the tank insulated top.

Additional simulations were realized to investigate the geometrical and operational effects of the finned tube such as fin diameter, thickness, material, and temperature of the cooling fluid.

4.2 EFFECT OF THE FIN DIAMETER

The effect of the fin diameter on the solidified mass fraction is shown in Fig. 9. As can be seen increasing the fin diameter increases the heat transfer area, increases the interface velocity and the solidified mass fraction and consequently reduces the time for complete solidification. The results in Fig. 10 confirm the reduction of the time for complete solidification with increase of the fin diameter expressed as Df/Dw.
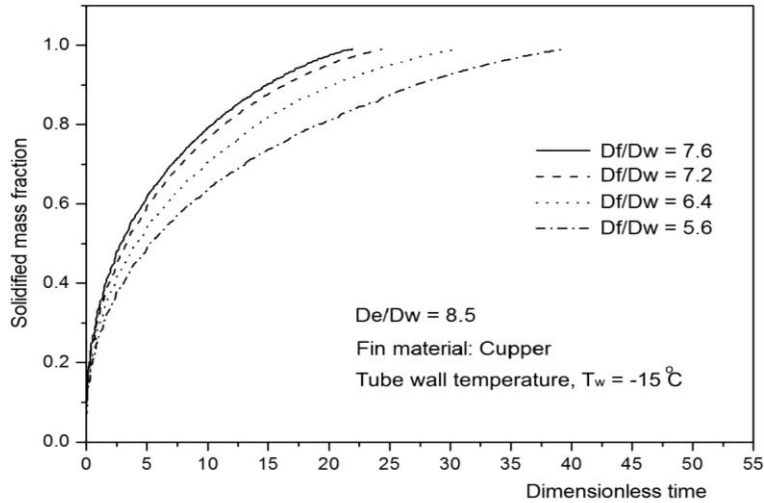
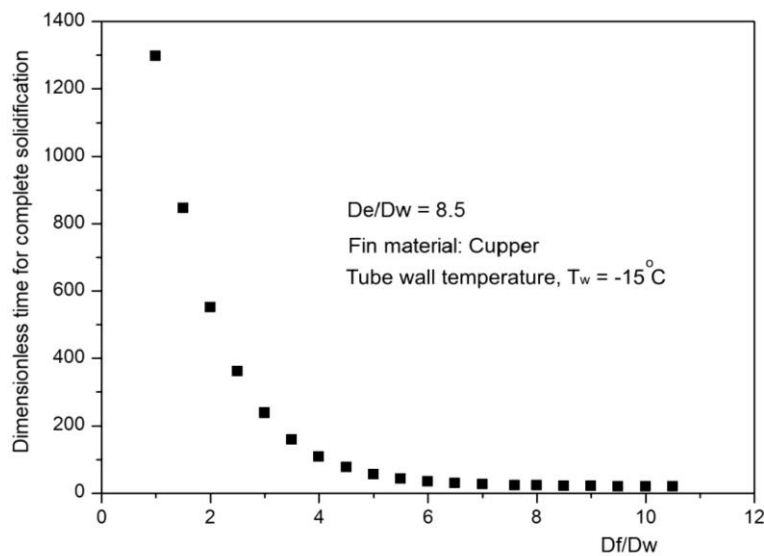Fig. 9 Effect of variation of the ratio D_f/D_w on the solidified mass fraction.

Fig. 10 Effect of variation of the ratio D_f/D_w on the dimensionless time for complete solidification.

4.3 EFFECT OF THE FIN THICKNESS

The influence of the fin thickness on the solidified mass fraction is shown in Fig. 11. As can be observed increasing the fin thickness produces a marginal increase of the solidified mass fraction and decreases the time for complete solidification as confirmed by the results shown in Fig. 12.
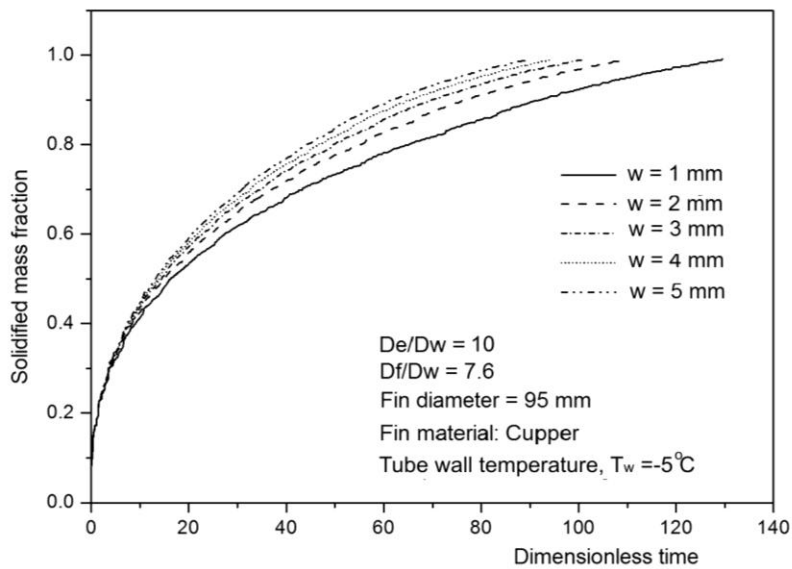
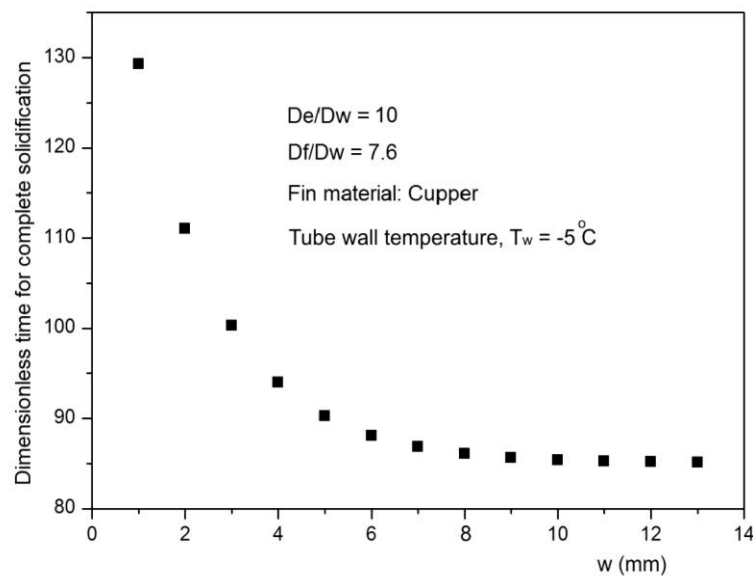Fig. 11 Effect of variation of the fin thickness on the solidified mass fraction.

Fig. 12 Effect of variation of the fin thickness on the dimensionless time for complete solidification.

4.4 EFFECT OF THE TEMPERATURE OF THE COOLING FLUID

The effect of the cooling fluid temperature on the solidified mass fraction is shown in Fig. 13. As can be seen reducing the cooling fluid temperature increases the temperature gradient between the PCM and the finned tube surface and this increases the interface velocity, increases the solidified mass fraction and reduces the time for complete solidification. Fig.14 confirms this conclusion.
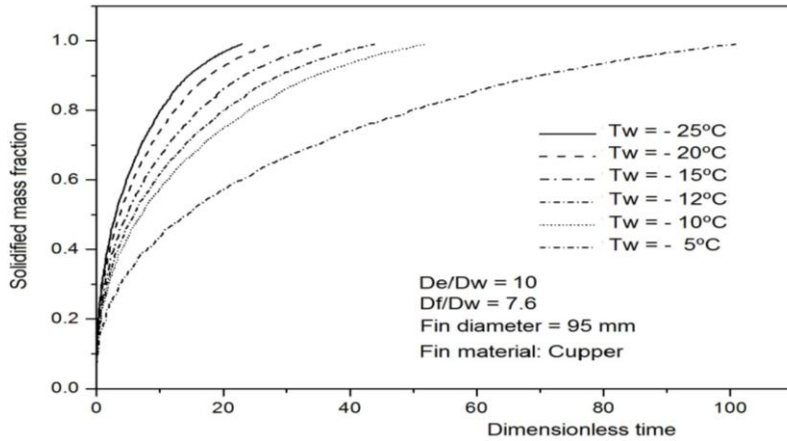
Fig. 13 Effect of variation of the temperature of the cooling fluid on the solidified mass fraction.
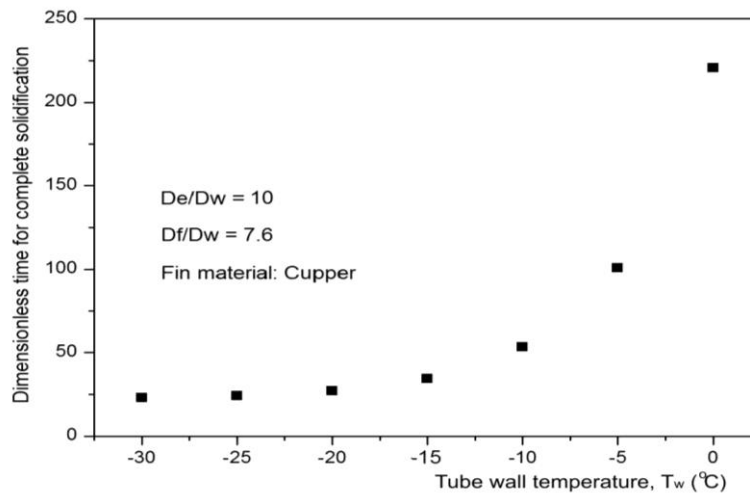

Fig. 14 Effect of variation of the temperature of the cooling fluid on the dimensionless time for complete solidification.

4.5 EFFECT OF THE FIN MATERIAL

The effect of the fin material on the solidified mass fraction is shown in Fig. 15. As can be expected metallic finned tubes good thermal conductors increasing the heat transfer rate, increasing the interface velocity and reducing the time for complete solidification.
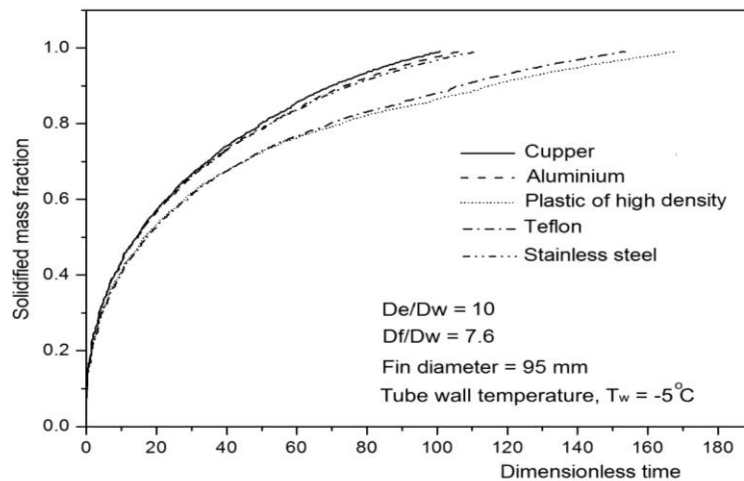

Fig. 15 Effect of variation of the fin material on the solidified mass fraction.

4.6 COMPARISON WITH THE BARE TUBE

In order to show explicitly the effect of incorporating fins on the tube submersed in PCM, additional experiments were realized with finless tube and the results were compared with the results of finned tube as in Fig. 16 which shows the variation of the interface velocity with time. One can observe the beneficial effect of the fins on enhancing the interface velocity. Fig. 17 shows a similar result for a temperature of the cooling fluid of -16 ^{o}C.
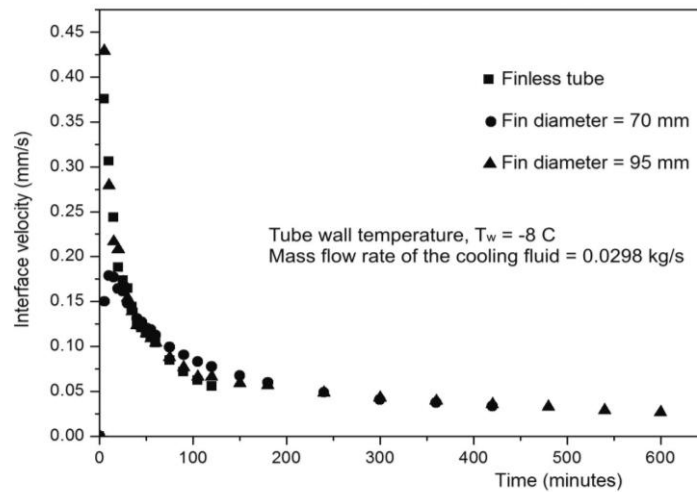
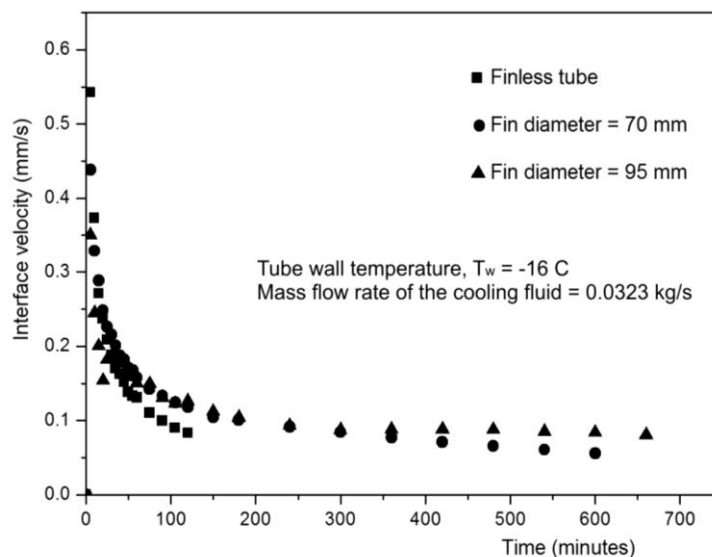Fig. 16 Experimental interface velocity for finned and finless tubes.

Fig. 17 Experimental interface velocity for finned and finless tubes.

Fig. 18 shows a comparison with the bare tube of the instantaneous interface position. As can be seen finned tubes show advanced interface position and hence more solidified mass fraction than the bare tube. Also from Fig. 19 one can observe that the increase of the fin diameter increases the solidified mass as explained before.
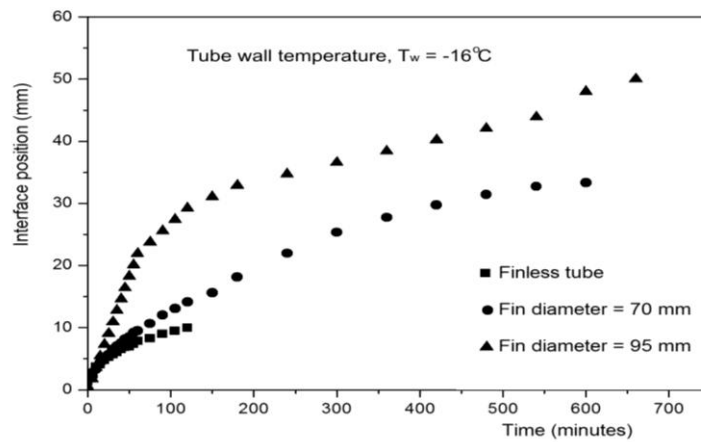
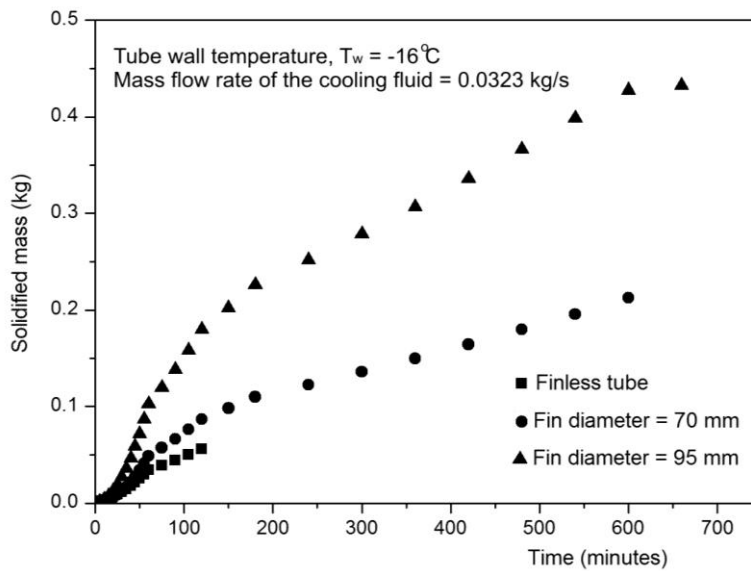Fig. 18 Experimental interface position for finned and finless tubes.

Fig. 19 Experimental solidified mass for finned and finless tubes.

Fig. 20 shows the energy stored in the cases of bare and finned tubes. As can be seen the fins strongly enhance the stored energy and renders the tube elements highly efficient.
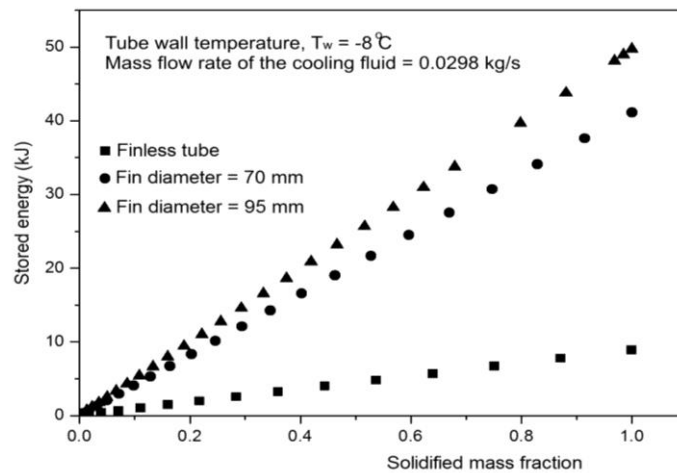

Fig. 20 Experimental stored energy for finned and finless tubes.

V.   CONCLUSIONS

In the present study a model is developed for the solidification of PCM around a tube with radial fin and was validated against experimental measurements. The numerical predictions and the experimental measurements revealed that increasing the fin diameter increases the interface velocity and reduces the time for complete solidification. Reducing the temperature of the cooling fluid enhances the interface velocity and reduces the time for complete solidification. The fin thickness appears to have little influence on the interface velocity or the time for complete solidification. Metallic fins seem to enhance the solidification process increasing the interface velocity and reducing the solidification time.

Few remarks are important to avoid misusing the present results. First of all the symmetry radius should be larger than the fin radius to avoid inefficiency of the process. The cooling fluid temperature should not be too low to avoid inefficiency of the refrigeration machine, a compromise between the low temperature and the solidification time should be established. Finally it is attractive to have finned tubes due to their good thermal performance. The cost of fabricating these tubes is relatively high due to the soldering process. An alternative solution is to use plastic tubes with impregnated metallic powder to improve their effective thermal conductivity. This at the moment is under development in our laboratory.

VI.   ACKNOWLEDGEMENTS

VII.   NOMENCLATURE

c	Specific heat [J kg^{-1}K^{-1}]
C	Heat capacity per unit volume = ρc [J m^{-3} K]
$\overline{C}(T)$	Heat capacity per unit volume including the phase change [J m^{-3} K]
H	Enthalpy per unit volume [J m^{-3}]
k	Thermal conductivity [W m^{-1} K^{-1}]
$\overline{k}(T)$	Thermal conductivity including the phase change [W m^{-1} K^{-1}]
L	Latent heat [J kg^{-1}]
r	Radial coordinate [m]
R	Dimensionless radial coordinate = r / r_w
rw	External radius of the tube [m]
ri	Internal radius of the tube [m]
re	Radius of external cylinder or radius of the symmetry circle [m]
rs	Radial position of the solid / liquid interface [m]
s(t)	Interface position [m]
T	Temperature [K]
Tm	Phase change temperature [K]
Tw	Tube wall temperature [K]
z	Axial coordinate [m]
Z	Dimensionless axial coordinate= z / r_w

Greek letters

δ	Dirac delta function
ΔT	Half the phase change temperature range [K]
ϕ	Dimensionless temperature
η	Unit function
λ	Latent heat per unit volume [J m-3]
ρ	Density [kg m-3]
τ	Dimensionless time = $k_s t / r_w c_s$
ξ	Dimensionless phase change temperature range = $(\Delta T)/(T_m - T_w)$

Subscripts

f	fin
ℓ	liquid

s   solid
w   wall

Abbreviations
PCM   Phase Change Material
ADI   Alternating Direction Implicit

REFERENCES

[1]   R. H. Henze and J. A. C. Humphrey, Enhanced heat conduction in phase-change thermal energy storage devices, Int. Journal Heat Mass Transfer, 24, 1981, 459-474.

[2]   P. V. Padmanabhan and M. V. K. Murthy, Outward phase change in a cylindrical annulus with axial fins on the inner tube, In. J. Heat Mass Transfer, 29 (12), 1986, 1855-1868.

[3]   K. A. R. Ismail, C. L. F. Alves, and M. S. Modesto, Numerical and experimental study on the solidification of PCM around a vertical axially finned isothermal cylinder, Applied Thermal Engineering, 21 (1), 2001, 53–77.

[4]   K. A. R. Ismail and M. G. E. Silva, Numerical solution of the Phase change problem around a horizontal cylinder with convection in the melt region, Int. Journal of Heat and Mass Transfer, 46 (10), 2003, 1791-1799.

[5]   Z. Liu, X. Sun, C. Ma, Experimental investigations on the characteristics of melting processes of stearic acid in an annulus and its thermal conductivity enhancement by fins, Energy Conversion and Management, 46, 2005, 959–969.

[6]   N. Kayansayan, M. A. Acar, Ice formation around a finned-tube heat exchanger for cold thermal energy storage, Int. Journal of Thermal Sciences, 45, 2006, 405–418.

[7]   N. Yuksel, A. Avci and M. Kilicn, A model for latent heat energy storage systems, Int. J. Energy Research, 30, 2006, 1146–1157.

[8]   S. Jegadheeswaran, S. D. Pohekar, Energy and exergy analysis of particle dispersed latent heat storage system, Int. Journal of Energy and Environment, 1 (3), 2010, 445-458.

[9]   K. Chintakrinda, R. D. Weinstein and A. S. Fleischer, A direct comparison of three different material enhancement methods on the transient thermal response of paraffin phase change material exposed to high heat fluxes, Int. Journal of Thermal Sciences, 50, 2011, 1639-1647.

[10]   M. R. Anisur, M. H. Mahfuz, M. A. Kibria, R. Saidur, I. H. S. C. Metselaar, T. M. I. Mahlia, Curbing global warming with phase change materials for energy storage, Renewable and Sustainable Energy Reviews, 18, 2013, 23–30.

[11]   M. Rahimi, A. A. Ranjbar, D. D. Ganji, K. Sedighi, and M. J. Hosseini, Experimental investigation of phase change inside a finned-tube heat exchanger, Hindawi Publishing Corporation Journal of Engineering, 2014, Article ID 641954, 11 pages, http://dx.doi.org/10.1155/2014/641954.

[12]   K. A. R. Ismail, M. M. Gonçalves and F. A. M. Lino, A parametric study of solidification of PCM in an annulus with alternating fins, Int. Journal of Research in Engineering and Advanced Technology, 3 (4), 2015, 188-202, August-September.

[13]   K. A. R. Ismail, M. M. Gonçalves and F. A. M. Lino, Solidification of PCM around a finned tube: modeling and experimental validation, Journal of Basic and Applied Research International, 12 (2), 2016, 115-128.

[14]   C. .Bonacina, G. Comini, A. Fasano, M. Primiceiro, Numerical solutions of phase change problems, Int. Journal Heat and Mass Transfer, 16 (15), 1973, 1825-1832.